

The north-south asymmetry of the interplanetary magnetic helicity generator function

Charles W. Smith and John W. Bieber

Bartol Research Institute, University of Delaware, Newark

Abstract. Previous analyses of the north-south asymmetry of the interplanetary magnetic helicity using the omnitape dataset have shown that there exists a persistent and statistically significant asymmetry in the helicity at 1 AU. The asymmetry is concentrated in fluctuations with spacecraft frame timescales less than 30 hours. We have extended these analyses to include data collected in the outer heliosphere where we are required to consider spacecraft frame timescales significantly greater than 30 hours. This shift in timescales is consistent with the rotation of the Parker spiral. We show the results from our studies of the Pioneer 10 & 11 datasets which demonstrate a north-south asymmetry of the magnetic helicity consistent with that seen in the inner heliosphere. Suggestive evidence of the selective decay of magnetic helicity is also presented. The asymmetry between the magnetic helicity of the two hemispheres has significant and measurable implications for cosmic ray propagation and these implications are reviewed briefly in light of the new results.

Introduction

The magnetic helicity is one of the invariants of incompressible MHD turbulence under prescribed boundary conditions [Woltjer, 1958] and represents the degree of linkage, or ‘knottedness’ of the magnetic field lines [Moffatt, 1978]. Since magnetic helicity can also represent the polarization of magnetic waves [Matthaeus and Goldstein, 1982], it affects charged-particle scattering when the polarization removes a significant fraction of the magnetic fluctuation energy from participating in the pitch-angle scattering by resonant interaction [Haselmann and Wibberenz, 1968]. Magnetic helicity, acting in concert with adiabatic focusing, can alter the parallel mean free path and convection speed of energetic charged particles in a manner that is dependent upon particle charge sign and the sun’s magnetic polarity [Bieber *et al.*, 1987; Bieber and Burger, 1990].

Bieber *et al.* [1987] show that the net magnetic helicity (integrated over wavenumber) of the interplanetary fluctuations responsible for the scattering of cosmic rays at 1 AU possesses a definite dominant sign which is predominantly negative north of the heliospheric current sheet and positive south of the sheet. Smith and Bieber [1993] show that this statistically significant net helicity resides at spatial scales corresponding to lags in the correlation function up to 30 hours and frequencies in the helicity spectrum less than 10^{-5} Hz. Escape of helicity-containing toroidal flux from the solar interior has been postulated by Bieber and Rust [1995a,b] as a possible source for magnetic helicity in the solar wind.

Matthaeus *et al.* [1990] and Bieber *et al.* [1993; 1994; 1995] show evidence derived from both direct observations of the correlation function for IMF fluctuations and cosmic ray propagation in the interplanetary medium suggesting that the true geometry of the IMF turbulence is a slab/2-D composite dominated in energy by the 2-D component. In this circumstance, most or all of the helicity would likely reside in the slab component [Smith and Bieber, 1993]. Because it is primarily the slab component that scatters the particles, the measured helicity as a fraction of the total turbulence energy may greatly underestimate the true contributions of helicity to particle scattering.

Analysis

Matthaeus and Smith [1981] and Matthaeus *et al.* [1982] provide a method for measuring the magnetic helicity, H_M , and its spectrum in interplanetary space using a single spacecraft. The magnetic helicity is defined by

$$H_M \equiv \int_0^{+\infty} \Phi(x) dx \quad (1)$$

where the generator function for the magnetic helicity is given by

$$\Phi(x) \equiv -[R_{yz}(x, 0, 0) - R_{zy}(x, 0, 0)] \quad (2)$$

and

$$R_{ij}(\mathbf{r}) \equiv \langle \delta B_i(\mathbf{x}) \delta B_j(\mathbf{x} + \mathbf{r}) \rangle. \quad (3)$$

R_{ij} is the correlation matrix for the magnetic fluctuations. Brackets $\langle \rangle$ denote ensemble average.

We separate measurements of the IMF into toward and away sector samplings according to the orientation of the hourly averaged data points used in this analysis and the predicted orientation of the IMF as derived from the Parker [1958] theory and the observed solar wind speed. In order to examine measurements recorded by the Pioneer 10 & 11 spacecraft at varying heliocentric distances without giving undue statistical weight to the inner-heliospheric measurements where the IMF fluctuation energy is greatest, we redefine $\Phi(x)$ to be

$$\tilde{\Phi} \equiv -[\tilde{R}_{yz}(x, 0, 0) - \tilde{R}_{zy}(x, 0, 0)] \quad (4)$$

where

$$\tilde{R}_{ij}(\mathbf{r}) \equiv \frac{\langle \delta B_i(\mathbf{x}) \delta B_j(\mathbf{x} + \mathbf{r}) \rangle}{\langle \sum_i \delta B_i(\mathbf{x}) \delta B_i(\mathbf{x}) \rangle}. \quad (5)$$

The term $\langle \sum_i \delta B_i(\mathbf{x}) \delta B_i(\mathbf{x}) \rangle$ is the average energy of the fluctuations within the interval which we subsequently denote as E_B . Such normalized correlation functions were computed for each solar rotation interval

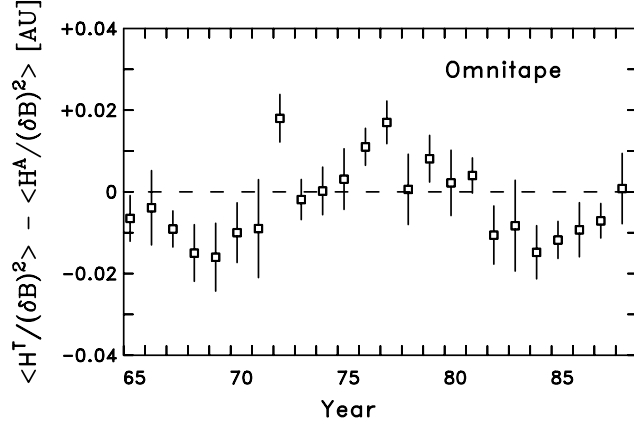


Figure 1. Yearly averages of net magnetic helicity difference between toward and away sector populations as recorded on the omnitape and computed using the energy-normalized analysis. The south-north asymmetry is achieved by reversing the signs on yearly values prior to 1969 and after 1981 and discarding years 1969-71 and 1980.

in the dataset. These can then be further averaged to yield estimates of $\tilde{\Phi}(x)$ so that averages over a range of heliocentric distances may be computed without giving undue emphasis to the inner heliospheric measurements. The trace of the energy-normalized correlation matrix, $\sum_i \tilde{R}_{ii}(r=0)$, is 1. The analyses of omnitape data performed previously [Bieber *et al.*, 1987; Smith and Bieber, 1993] have been repeated to verify the validity of this approach.

Figure 1 uses the energy-normalized analysis to reproduce the yearly difference in the toward and away sector net magnetic helicity demonstrated by Bieber *et al.* [1987]. Except for a general and approximate renormalization of the helicity by the average energy of the sectors, the results are in good agreement with the earlier treatment. Separation into toward and away sector populations removes the energy associated with sector crossings, but leaves other large-scale transients to contribute to the energy. Intermediate-scale analyses of the correlation functions computed over individual solar rotations provide statistically independent estimates of the correlation function and magnetic helicity generating function which can be averaged further. The net energy-normalized helicity demonstrates the relative amount of helicity vs. energy contained in the solar wind fluctuations. From this a persistent difference in the net magnetic helicity of the northern and southern hemispheres may be deduced with the southern hemisphere having a greater magnetic helicity than the north.

Figure 2 (top panel) shows the separate northern and southern hemispheric values of $\tilde{\Phi}$ as computed from the omnitape dataset using the above energy-normalized analysis for the combined years of 1965 through 1988. The values of $\tilde{\Phi}$ for the northern and southern hemispheres ($\tilde{\Phi}^N$ and $\tilde{\Phi}^S$) differ in sign, but otherwise dis-

play similar forms. Values of $\tilde{\Phi}^N$ and $\tilde{\Phi}^S$ computed from the PVO dataset are similar in form. Although not shown, the energy-normalized analysis of the helicity remains true to the more familiar method except for an overall renormalization consistent with the average energy. The south-north difference of $\tilde{\Phi}$ derived from the omnitape is shown in Figure 2 (bottom panel). The magnetic helicity asymmetry at 1 AU (and 0.7 AU although it is not shown) resides in time-scales (length-scales) less than ~ 30 hours ($\sim 5 \times 10^7$ km). At greater lags, $\tilde{\Phi}$ approaches zero and varies in a random fashion. Convergence of $\tilde{\Phi}$ to zero indicates that the magnetic helicity is correctly determined with maximum lags in excess of 30 hours in so far as convergence of $\tilde{\Phi}$ at long lags is required by the analysis [Matthaeus and Smith, 1981; Matthaeus *et al.*, 1982]. The difference $\tilde{\Phi}^S - \tilde{\Phi}^N$ does not result from like-signed functions that differ in magnitude.

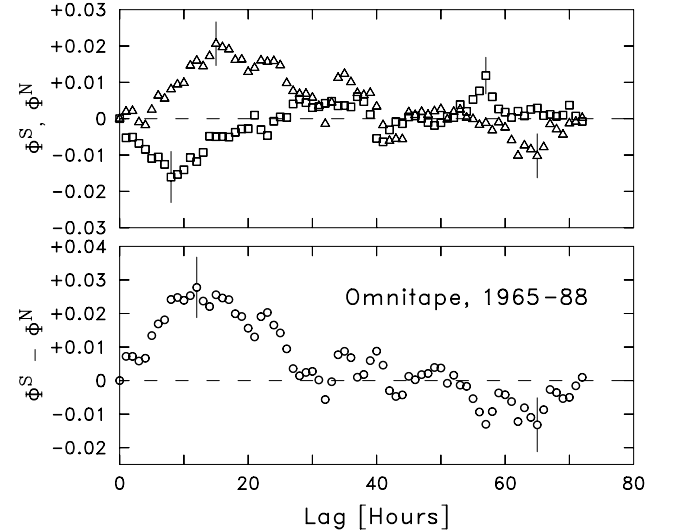


Figure 2. (Top panel) $\tilde{\Phi}(r)$ for northern (squares) and southern (triangles) hemispheres as computed from omnitape dataset. (Bottom panel) South-north difference of correlation functions. The net energy-normalized magnetic helicity is given by the integral over these correlation functions.

We can use Figure 2 to compute a 24-year average of the energy-normalized helicity for the northern and southern hemispheres as well as the helicity asymmetry by summing over lags according to:

$$\langle H_M^S/E_B^S \rangle = \sum_i \tilde{\Phi}^S(r_i) \Delta r \quad (6)$$

$$\langle H_M^N/E_B^N \rangle = \sum_i \tilde{\Phi}^N(r_i) \Delta r \quad (7)$$

where $\Delta r = V_{sw} \times (1\text{hr})$. The net south-north energy-normalized magnetic helicity asymmetry derived from the omnitape measurements for the years 1965 through 1988 as computed for lags up to 72 hours is 0.0041 ± 0.0007 AU. The northern and southern hemispheric values are -0.0008 ± 0.0005 AU and 0.0033 ± 0.0005 AU,

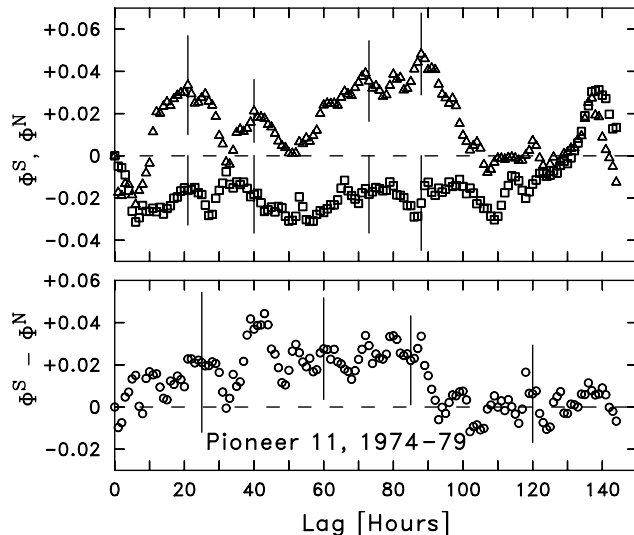


Figure 3. (Top panel) $\tilde{\Phi}(r)$ for northern (squares) and southern (triangles) hemispheric measurements recorded by Pioneer 11 from 1974 through 1979. (Bottom panel) South-north difference of $\tilde{\Phi}$.

respectively. Uncertainties here and throughout the paper are the computed error of the mean. Both means and uncertainties are derived from the ensemble of solar rotation averages.

We have examined measurements recorded by Voyager 1 & 2 and Pioneer 10 & 11 from 1974 through 1989 spanning heliocentric distances from 1 to 45 AU. The analyses show a general trend for non-zero values in $\tilde{\Phi}$ to move toward larger lags as we show below.

The computed values of $\tilde{\Phi}^N$ and $\tilde{\Phi}^S$ derived from Pioneer 11 observations from 1974 through 1979 spanning heliocentric distances from 1 to 9 AU are shown in Figure 3 (top panel). These curves possess the same general form displayed by the omnitape and PVO results except that there is less statistical significance owing to the shorter data set, and the lag at which the correlation functions converge to zero is longer. The south-north difference of $\tilde{\Phi}$ shown in the bottom panel of Figure 3 demonstrates a nearly positive-definite value for lags less than 100 hours in keeping with the 1 AU result and the general rotation of the IMF to greater winding angles. If all else is constant in a slab geometry, then rotation of the mean magnetic field from $\Psi_{winding} \simeq 45^\circ$, which is typical of Earth-orbit measurements, to $\Psi_{winding} \simeq 78^\circ$, which approximately typifies this dataset, corresponds to spatial structures which appear at 30 hour lags now becoming apparent at 100 hour lags.

Figure 4 repeats the same analysis as before for Pioneer 10 measurements recorded from 1972 through 1975 and from 1 to 8.4 AU. It demonstrates less clear results for the separate northern and southern hemispheres, but the bottom panel demonstrates that $\tilde{\Phi}^S$ tends to contain estimates larger in value than the northern fields, resulting in a positive south-north asymmetry.

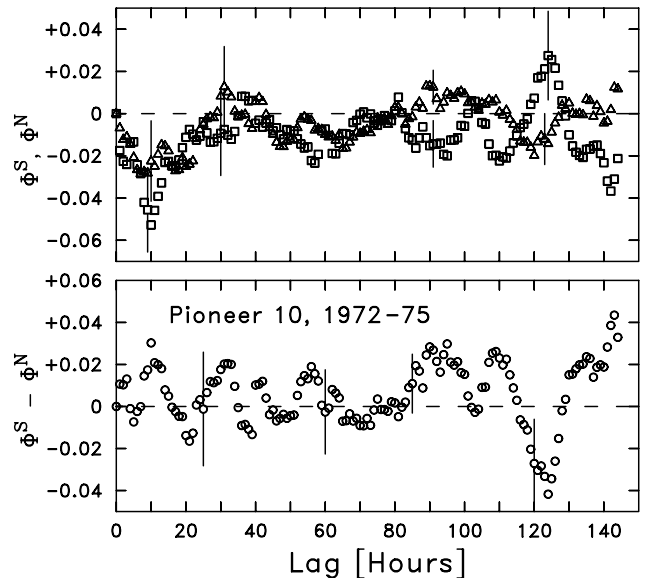


Figure 4. (Top panel) $\tilde{\Phi}(r)$ for northern (squares) and southern (triangles) hemispheric measurements recorded by Pioneer 10 from 1972 through 1975. (Bottom panel) South-north difference of $\tilde{\Phi}$.

The shorter time period also offers less statistical significance to the estimates.

We can compute the net helicity from the Pioneer 10 & 11 correlation functions shown above as well as for the omnitape over the same time periods and for the same maximum lag. These values are tabulated in Table 1. Both the northern and southern hemispheric measurements demonstrate an increased ratio of H_M/E_B in the outer heliosphere relative to 1 AU with the exception of the Pioneer 10 measurements of the southern hemisphere. The helicity asymmetry is divided on this issue due to the Pioneer 10 southern hemispheric measurements. Although 3 out of 4 results offer suggestive evidence of selective decay [Matthaeus and Montgomery, 1980], more study is needed before either selective decay or inverse cascade processes can be claimed.

Summary

A persistent difference exists between magnetic helicity measurements made north and south of the heliospheric current sheet. This asymmetry is observed to persist from 1 to 9 AU. The net magnetic helicity of the southern hemisphere is consistently greater than that of the northern hemisphere with oppositely signed helicity at the large scales. In the inner heliosphere the net magnetic helicity resides at length-scales associated with 30 hour lags ($\sim 5 \times 10^7$ km).

This analysis indicates that the north-south asymmetry of the magnetic helicity seen within the inner heliosphere persists and increases slightly in the outer heliosphere. The length scale at which consistently non-zero levels of magnetic helicity are observed increases

Table 1. Helicity Length Scales

Dataset	Years	$\langle H_M^S/E_B \rangle$ [AU]	$\langle H_M^N/E_B \rangle$ [AU]	$\langle \frac{H_M^S}{E_B} \rangle - \langle \frac{H_M^N}{E_B} \rangle$ [AU]
omnitape	1965-88	0.004 ± 0.001	-0.007 ± 0.001	0.011 ± 0.001
omnitape	1972-75	0.009 ± 0.002	-0.012 ± 0.002	0.022 ± 0.003
Pioneer 10	1972-75	-0.007 ± 0.002	-0.016 ± 0.002	0.008 ± 0.003
omnitape	1974-79	0.002 ± 0.002	-0.005 ± 0.002	0.007 ± 0.003
Pioneer 11	1974-79	0.020 ± 0.003	-0.011 ± 0.002	0.031 ± 0.003

with heliocentric distance according to the winding angle of the large-scale IMF, in a manner consistent with the helicity residing in the slab geometry component of the IMF fluctuations.

There are several reasons to believe that the geometry of the IMF fluctuations is a composite of slab and 2-D [Matthaeus *et al.*, 1990; Oughton *et al.*, 1994; Bieber *et al.*, 1994]. Transverse 2-D turbulence cannot contain magnetic helicity. If the solar turbulence has a dominant 2-D component, as recent evidence suggests, then the significance of helicity in the minority component is elevated correspondingly.

The analysis of the two intervals of Pioneer data suggest that selective decay or inverse cascade of magnetic helicity may be operating in the solar wind. Many processes, including the injection of helical energy by stream-stream interaction [Zank *et al.*, 1995], could possibly account for the observation as well. This result is only preliminary at present.

We have examined the Voyager dataset and other years of Pioneer measurements as well with mixed results. While the suggestion that helicity moves to longer lags is generally upheld, the correlation functions generally degrade due to a lack of statistical significance brought on by sampling problems. These problems are thought to result from the increased winding angle at large heliocentric distances as well as the movement of the spacecraft through a decidedly non-stationary and inhomogeneous IMF. Efforts to overcome these problems are ongoing.

Acknowledgments. Support for this work was provided by NASA grant NAGW-3033, NSF grant ATM-9314683 and the NASA Space Physics Theory Program grant to the Bartol Research Institute. Data was provided by N. F. Ness, C. T. Russell, E. J. Smith, and the National Space Science Data Center. Discussions with W. H. Matthaeus are gratefully acknowledged.

References

- Bieber, J. W., and R. Burger, Cosmic-ray streaming in the Born approximation, *Astrophys. J.*, **348**, 597-607, 1990.
- Bieber, J. W., and D. M. Rust, The escape of magnetic flux from the Sun, *Astrophys. J.*, in press, 1995a.
- Bieber, J. W. and D. M. Rust, Escape of magnetic toroids from the Sun, these proceedings, 1995b.
- Bieber, J. W., P. Evenson, and W. H. Matthaeus, Magnetic helicity of the IMF and the solar modulation of cosmic rays, *Geophys. Res. Lett.*, **14**, 864-867, 1987.
- Bieber, J. W., W. H. Matthaeus, and C. W. Smith, A turbulence theory solution of the quasilinear theory puzzle, *Proc. 23rd Internat. Cosmic Ray Conf.* (Calgary), **3**, 211-214, 1993.
- Bieber, J. W., W. H. Matthaeus, C. W. Smith, W. Wanner, M.-B. Kallenrode, and G. Wibberenz, Proton and electron mean free paths: The Palmer consensus revisited, *Astrophys. J.*, **420**, 294-306, 1994.
- Bieber, J. W., W. Wanner, and W. H. Matthaeus, Dominant 2D magnetic turbulence in the solar wind, these proceedings, 1995.
- Goldstein, M. L., and W. H. Matthaeus, The role of magnetic helicity in cosmic ray transport theory, *Proc. 17th Internat. Cosmic Ray Conf.*, **3**, 294-297, 1981.
- Hasselmann, K. and G. Wibberenz, Scattering of charged particles by random electromagnetic fields, *Zs. Geophys.*, **34**, 353-388, 1968.
- Matthaeus, W. H., and D. C. Montgomery, Selective decay hypothesis at high mechanical and magnetic Reynolds numbers, in *Nonlinear Dynamics*, Annals of The New York Academy of Sciences, **357**, edited by R. H. G. Helleman, pp. 203-222, New York Academy of Sciences, New York, 1980.
- Matthaeus, W. H., and C. W. Smith, Structure of correlation tensors in homogeneous anisotropic turbulence, *Phys. Rev.*, **A24**, 2135-2144, 1981.
- Matthaeus, W. H. and M. L. Goldstein, Measurement of the rugged invariants of magnetohydrodynamic turbulence in the solar wind, *J. Geophys. Res.* **87**, 6011-6028, 1982.
- Matthaeus, W. H., M. L. Goldstein, and C. W. Smith, Evaluation of magnetic helicity in homogeneous turbulence, *Physical Review Letters*, **48**, 1256-1259, 1982.
- Matthaeus, W. H., M. L. Goldstein, and D. A. Roberts, Evidence for the presence of quasi-two-dimensional nearly incompressible fluctuations in the solar wind, *J. Geophys. Res.*, **95**, 20,673-20,683, 1990.
- Moffatt, H. K., *Magnetic Field Generation in Electrically Conducting Fluids*, Cambridge University Press, New York, 1978.
- Oughton, S., E. R. Priest, and W. H. Matthaeus, The influence of a mean magnetic field on three-dimensional magnetohydrodynamic turbulence, *J. Fluid Mech.*, **280**, 95-117, 1994.
- Parker, E. N., Dynamics of the interplanetary gas and magnetic fields, *Astrophys. J.*, **128**, 664-676, 1958.
- Smith, C. W., and J. W. Bieber, Detection of steady magnetic helicity in low-frequency IMF turbulence, *Proc. 23rd Internat. Cosmic Ray Conf.* (Calgary), **3**, 493-496, 1993.
- Woltjer, L., A theorem on force-free magnetic fields, *Proc. Nat. Acad. Sci.*, **44**, 489-491, 1958.
- Zank, G. P., W. H. Matthaeus, and C. W. Smith, Evolution of turbulent magnetic fluctuation power with heliocentric distance, these proceedings, 1995.

C.W. Smith and J.W. Bieber, Bartol Research Institute, University of Delaware, Newark, DE 19716. (e-mail: chuck@bartol.udel.edu and john@bartol.udel.edu)